Chemistry–A European Journal
Research Article
doi.org/10.1002/chem.202104574
Chemistry Europe
European Chemical Societies Publishing
www.chemeurj.org

Quadrupolar Ultrafast Charge Transfer in Diaminoazobenzene-Bridged Perylenediimide Triads

Sairaman Seetharaman[+],[a] Nathalie Zink-Lorre[+],[b] David Gutiérrez-Moreno[+],[b] Paul A. Karr,[c] Fernando Fernández-Lázaro,*[b] and Francis D'Souza*[a]

Abstract: Strong push-pull interactions between electron donor, diaminoazobenzene (azo), and an electron acceptor, perylenediimide (PDI), entities in the newly synthesized A–D–A type triads (A = electron acceptor and D = electron donor) and the corresponding A–D dyads are shown to reveal wide-band absorption covering the entire visible spectrum. Electrochemical studies revealed the facile reduction of PDI and relatively easier oxidation of diaminoazobenzene in the dyads and triads. Charge transfer reversal using fluorescence-spectroelectrochemistry wherein the PDI fluorescence recovery upon one-electron oxidation, deterring the charge-transfer interactions, was possible to accomplish. The charge transfer state density difference and the frontier orbitals from the DFT calculations established the electron-deficient PDI to be an electron acceptor and diaminoazobenzene to be an electron donor resulting in energetically closely positioned $PDI^{\delta-}$-$Azo^{\delta+}$-$PDI^{\delta-}$ quadrupolar charge-transfer states in the case of triads and $Azo^{\delta+}$-$PDI^{\delta-}$ dipolar charge-transfer states in the case of dyads. Subsequent femtosecond transient absorption spectral studies unequivocally proved the occurrence of excited-state charge transfer in these dyads and triads in benzonitrile wherein the calculated forward charge transfer rate constants, k_f, were limited to instrument response factor, meaning $>10^{12}$ s^{-1} revealing the occurrence of ultrafast photo-events. The charge recombination rate constant, k_r, was found to depend on the type of donor-acceptor conjugates, that is, it was possible to establish faster k_r in the case of triads ($\sim 10^{11}$ s^{-1}) compared to dyads ($\sim 10^{10}$ s^{-1}). Modulating both ground and excited-state properties of PDI with the help of strong quadrupolar and dipolar charge transfer and witnessing ultrafast charge transfer events in the studied triads and dyads is borne out from the present study.

Introduction

Supramolecular donor-acceptor conjugates appended with different electron and energy donors and acceptors have attracted tremendous interest over the past decades for their applications in solar light harvesting, spintronics, and quantum information science.[1–3] Interestingly, when a strong electron donor and an electron acceptor are directly connected, due to the phenomenon of intramolecular charge polarization and charge transfer, modulation of both ground and excited state spectral properties occur, often resulting in new emission peaks of charge transfer origin.[4] Advantageously, the occurrence of such charge transfer transitions would extend optical coverage which otherwise is restricted to the narrow transitions related to locally excited states of the entities.

Perylenediimides (PDI) are highly colored, thermally and photochemically stable dyes, widely used in industrial applications, for example, high-grade pigments in automotive finishes.[5] Importantly, PDIs have emerged as a valuable material for organic electronics, and as versatile building blocks for functional optoelectronic architectures.[6] Other pertinent applications of PDI include dye material for contactless pH measurements, luminescent probes for metal ion and explosives sensing,[7] and performing different roles in organic and hybrid photovoltaics.[8] PDIs possess highly tailorable structures, versatile electronic and optical properties such as excellent electron affinity, strong optical absorption, remarkable monomeric fluorescence with near 100% quantum yields in solution, desirable excited state lifetimes, etc.[9] PDIs reveal absorption covering 420–550 nm, and fluorescence covering the 520–720 nm range, both with 2–3 vibrionic peaks.[9]

Azobenzene (azo), a diazene (HN=NH) derivative where both hydrogens are replaced by phenyl groups is known to undergo cis-to-trans structural change upon photo-irradiation.[10a–c] Consequently, they have been extensively used in the development of molecular-scale information storage, light-triggered switches, nonlinear optical guides, protein probes, molecular machines, and metal ion chelators.[10d–f] A

[a] Dr. S. Seetharaman,[+] Prof. Dr. F. D'Souza
Department of Chemistry
University of North Texas
1155 Union Circle, #305070, Denton, TX 76203-5017 (USA)
E-mail: Francis.DSouza@UNT.edu

[b] Dr. N. Zink-Lorre,[+] Dr. D. Gutiérrez-Moreno,[+] Prof. Dr. F. Fernández-Lázaro
Área de Química Orgánica, Instituto de Bioingeniería
Universidad Miguel Hernández
Avda. de la Universidad s/n, 03202 Elche (Spain)
E-mail: fdofdez@umh.es

[c] Prof. Dr. P. A. Karr
Department of Physical Sciences and Mathematics
Wayne State College
Wayne, Nebraska 68787 (USA)

[+] These authors contributed equally to this work.

Supporting information for this article is available on the WWW under https://doi.org/10.1002/chem.202104574

literature survey shows that although PDI has been used to build novel donor-acceptor constructs with appropriate donors, there is no report on coupling PDI with azobenzene at the bay positions that is capable of revealing strong charge-transfer interactions. The only recent report from our groups on a PDI-azo-PDI triad (the azo group was linked to PDI via phenoxy linkers) revealed very weak charge-transfer interactions between the PDI and azobenzene entities without significantly perturbing the spectral properties.[11,12]

As part of our continued effort to build highly interacting donor-acceptor conjugates revealing strong excited-state intramolecular charge transfer,[13] and knowing the above-mentioned novel properties of both PDI and azobenzene, in the present study, we have re-designed our approach of building PDI-azo-PDI acceptor-donor-acceptor triads. In the present approach instead of previously employed 4-phenoxy linkers, we have used 4-aminophenyl linkers, as shown in Figure 1. The presence of *p*-amino groups on the phenyl rings of azobenzene spacer made this entity electron-rich promoting strong charge-transfer interactions with the electron-deficient PDI entities (see structures in Figure 1). The modulated ground state spectral features and excited-state charge transfer events have been systematically probed by a suite of spectral, electrochemical, computational, and time-resolved spectroscopic studies, and summarized in the following section.

Results and Discussion

Scheme 1 illustrates the synthetic scheme for PDI-Azo-PDI, **Triad 1**, and **Triad 2**. In brief, **PDI 1, PDI 2**, and **Dyad 1** were prepared following the general procedure described elsewhere.[14] **Dyad 2**, **Triad 1**, and **Triad 2** were synthesized by a fluoride-mediated coupling of the appropriate aromatic amines with either **PDI 1** or **PDI 2.**[14b] The synthetic details and the NMR and mass spectral data of all new three compounds are given in the experimental section while pertinent NMR and mass data are shown in Figures S1–S9.

Figure 2a illustrates the absorption spectrum of representative **Triad 2** along with monomeric **PDI 1** control in benzonitrile.

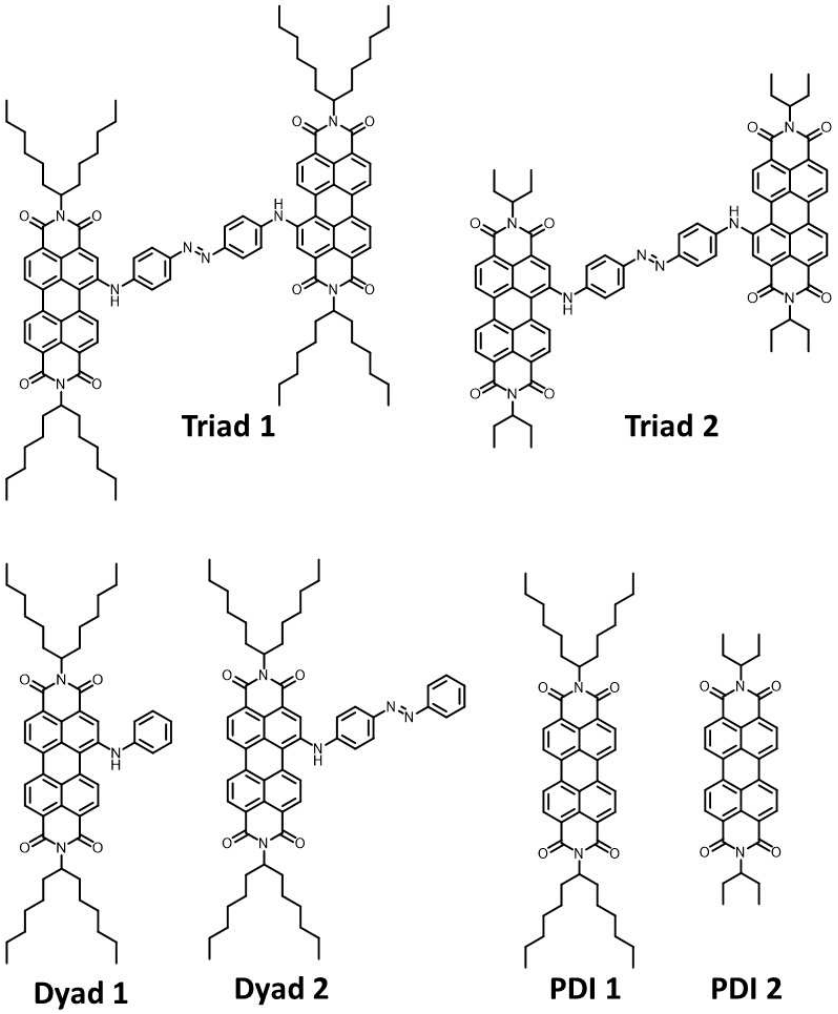

Figure 1. Structure of the PDI-azo-PDI triads, PDI-amino and PDI-aminoazobenzene dyads, and the control PDI monomers used in the present study to demonstrate wide-band light capture and subsequent excited-state charge transfer phenomenon.

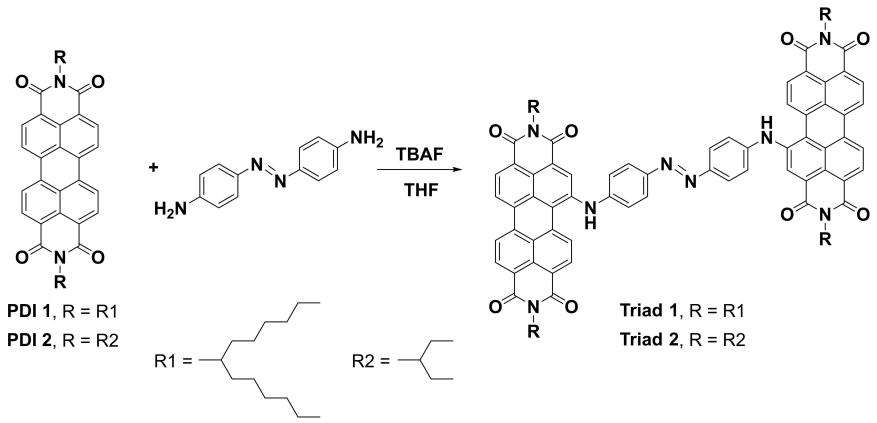

Scheme 1. Synthesis of aminoazobenzene-bridged PDI-Azo-PDI conjugates, **Triad 1** and **Triad 2**.

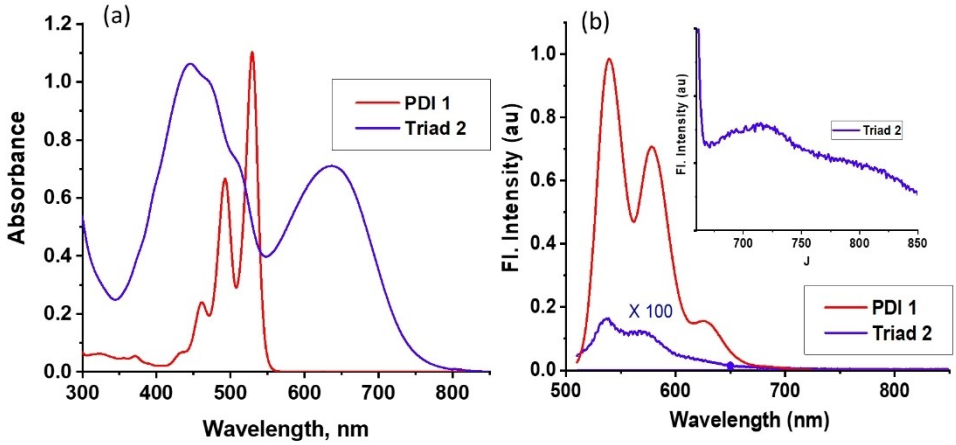

Figure 2. (a) Absorption and (b) fluorescence spectra of **PDI 1** monomer (red) and **Triad 2** (blue) in benzonitrile. The compounds were excited at 492 nm. Figure 2b inset shows the charge transfer emission of Triad 2 in the red region.

PDI 1 revealed absorption peaks at 435, 462, 492, and 535 nm, typical of monomeric PDI compounds.[15] Interestingly, **Triad 2** revealed two broad peaks centered around 447 and 639 nm. The optical coverage spanned the entire 300–800 nm range due to strong ground-state polarization and extended π-conjugation. Absorption spectra in benzonitrile of all the compounds displayed in Figure 1 are shown in Figure S10a while pertinent data are given in Table 1. While spectral features of **PDI 1** and **PDI 2** were typical of monomeric PDI,[15] **Dyad 1** functionalized with a secondary aminophenyl electron donor, and **Dyad 2** functionalized with an aminoazobenzene electron donor, both at the bay positions, and the second **Triad 1** with diaminoazobenzene bridge revealed broadband spectrum covering the entire visible region. The peak maxima for both triads were red-shifted by about 20 nm compared to the dyads suggesting slightly better spectral coverage from the A–D–A triads. Due to strong ground-state polarization, the absorption of azobenzene, expected in the 300–400 nm region,[12] was buried within the PDI peaks and could not be resolved. This precluded us to perform light-induced trans→cis isomerization for the present set of triads.

Table 1. Optical absorption and emission in CH_2Cl_2, and energies of charge-transfer states estimated from charge transfer emission peak maxima in benzonitrile.

Compound	Absorption: λ, nm (log ε)	Emission: λ, nm (τ, ns)	Φ_f	E_{CT}, eV
PDI 1	457 (4.6), 488 (5.0), 524 (5.2)	534, 571 (4.20)	1.00	–
PDI 2	457 (4.6), 488 (5.0), 524 (5.2)	534, 571 (4.27)	0.85	–
Dyad 1	449 (3.8), 606 (3.9)	532, 572	0.001	1.70
Dyad 2	392 (4.4), 484 (4.2), 593 (4.2)	528, 565	0.001	1.72
Triad 1	436 (4,7), 615 (4.5)	498, 534	0.002	1.60
Triad 2	435 (4.5), 608 (4.3)	551	0.001	1.73

The fluorescence spectra of **PDI 1** and **Triad 2** are shown in Figure 2b. Monomeric **PDI 1** revealed emission peaks at 540, 578, and 626 nm; however, the fluorescence of **Triad 2** was almost nonexistent. Very weak emission in the PDI monomer region (over 99% quenching) was observed; however, scanning the wavelength beyond the typical PDI emission region revealed a very weak, broad emission band with peak maxima

at 714 nm. This trend was also the case for the other **Triad 1** and the **Dyads 1** and **2**, as shown in Figure S10b inset. Monomeric **PDI 2** was highly fluorescent, however, **Dyad 1** having a directly linked amino group at the bay position was weakly fluorescent (88% quenching), and **Dyad 2**, having an amino-azobenzene at the bay position, was non-fluorescent (99% quenching). Similar to **Triad 2**, the emission of **Triad 1** was also non-existent. Extending the emission scan further, a near-IR charge transfer emission peak was obvious. For **Dyad 1** and **2**, the CT-emission was located at 731 and 723 nm, respectively. Interestingly, for **Triad 1**, the weak CT-emission peak further red-shifted and was located at 776 nm. These results conclusively prove strong charge-transfer interactions in the amino- and aminoazobenzene functionalized PDI dyads and triads in benzonitrile perturbing both ground and excited-state properties.[4] Lifetimes measured using single-photon counting revealed monoexponential decays for **PDI 1** and **PDI 2** with lifetimes of 4.20 and 4.27 ns, respectively (see Figure S11 for decay profiles). For the other compounds, due to very weak emission, accurate lifetimes were difficult to determine. The decay profiles overlapped with the instrument response function suggesting the lifetimes are less than 200 ps.

The singlet-singlet energies ($E_{0,0}$) were estimated from the 0,0 absorption and fluorescence peak maxima. For monomeric PDIs these were 2.31 eV; for dyads, values were ~2.16 eV, and for triads, the $E_{0,0}$ values were ~2.10 eV. Smaller $E_{0,0}$ due to the presence of amino azobenzene at the bay position was apparent from this study.

Electrochemical properties were subsequently investigated using cyclic and differential pulse voltammetry techniques. Representative voltammograms are shown in Figure S12 and the redox potentials are summarized in Table S1 in Supporting Information. Briefly, both **PDI 1** and **PDI 2** revealed two one-electron reductions and a one-electron oxidation process within the accessible potential window of benzonitrile. Interestingly, in the case of dyads and triads having either amino- or amino-azobenzene functionalized PDIs, additional oxidation before PDI oxidation was observed. For **Dyad 1** and **Dyad 2**, this process was located respectively at ~0.55 and 0.57 V vs. Fc/Fc^+ while for **Triad 1** and **Triad 2**, this process was at ~0.89 and 0.86 V, respectively. This new anodic process has been attributed to the oxidation of respective amino- and aminoazobenzene groups within the compounds. Consequently, the measured electrochemical redox gaps (difference between the first oxidation and first reduction) were smaller for PDI having amino- or aminoazobenzene functionalities compared to those lacking such functionality. This study brings out an important observation of the redox-active role of amino- and amino-azobenzene functionalities and their facile oxidation over PDI, and subsequently promotes the charge-transfer interactions.

We also attempted to reverse the charge transfer in the studied triads. That is, oxidation of the diaminoazobenzene functionality is expected to minimize the push-pull interactions by lowering the electron density on the diaminoazobenzene entity of the triads. If this happens then one would expect restoration of the quenched fluorescence of the triad.[16] This was found to be indeed the case as shown for representative **Triad 2** during fluorescence-spectroelectrochemistry. Figure 3 shows the spectral changes during the first oxidation of **Triad 2**. Recovery of fluorescence to some extent (~20%) was observed indicating charge transfer reversal in the studied triad. Lack of 100% fluorescence recovery could be attributed to the existence of low-energy excited states of the oxidized triad (see Figure S16) that could quench the fluorescence or radical nature of the oxidized species. In any case, the significance of fluorescence-spectroelectrochemistry to achieve charge transfer reversal was clear from this study.

To secure further insights on the electronic structure and the push-pull effects, computational studies were performed at the B3LYP/6-311G(d,p) level.[17] The structures were optimized completely on a Born-Oppenheimer potential energy surface. Optimized structures along with frontier orbitals of the triads are shown in Figure S13. In these systems, the diaminoazobenzene spacer having a C_{2h} symmetry was almost orthogonal to the PDI entities of the triad. The two PDI entities were almost in the same plane with a center-to-center distance of ~10 Å and dihedral between PDI planes of about 10°. Figures 4a and b show the frontier HOMO and LUMO of **Triad 1**. The majority of the HOMO was on the diaminoazobenzene with some contributions on the PDI entity. Likewise, the LUMO was almost completely on the PDI entities. Figures 4c and d show electrostatic potential surfaces of the S_1 and S_2 states (difference between the ground and the corresponding excited state). The red and blue colors, respectively, show the electron density of the electron donor and electron acceptor regions. Collectively, these results suggest both excited S_1 and S_2 states of PDI to participate in the CT process resulting in $PDI^{\delta-}$-$Azo^{\delta+}$-$PDI^{\delta-}$ quadrupolar charge transfer states. Calculations on **Dyad 2** also revealed such results as shown in Figure S14. The electrostatic potential surfaces of the S_1 and S_2 states suggest $PDI^{\delta-}$-$Azo^{\delta+}$ dipolar charge transfer in this dyad.

An energy diagram was subsequently established using the spectral data as shown in Figure 5. The thermodynamic feasibility of charge transfer events in benzonitrile was obvious

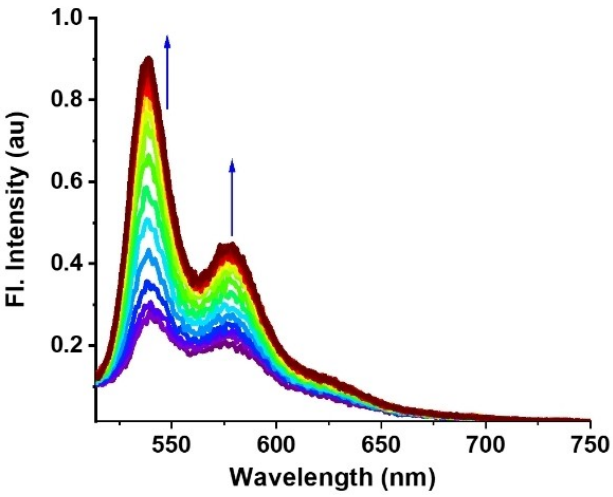

Figure 3. Fluorescence-spectroelectrochemical changes of **Triad 2** during first oxidation in benzonitrile containing 0.2 M $(TBA)ClO_4$.

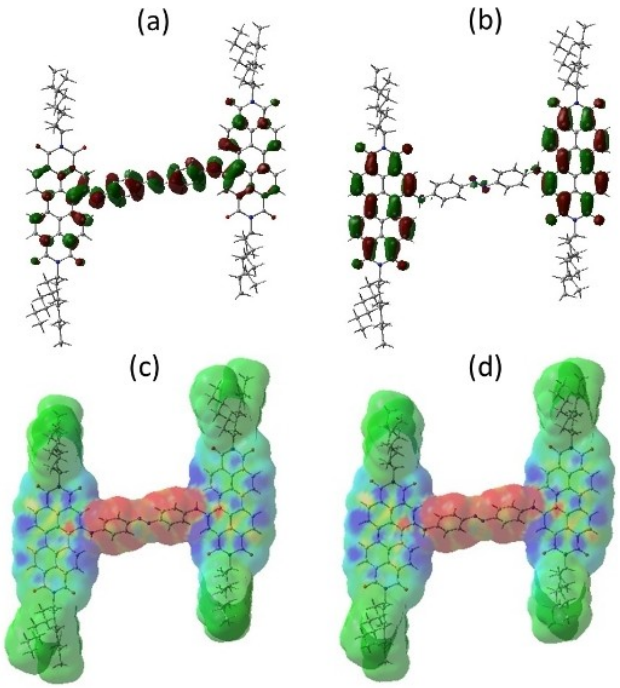

Figure 4. Frontier (a) HOMO, (b) LUMO, electrostatic potential map for (c) S_1 and (d) S_2 states on B3LYP/6-311G(d,p) optimized structure of **Triad 1**.

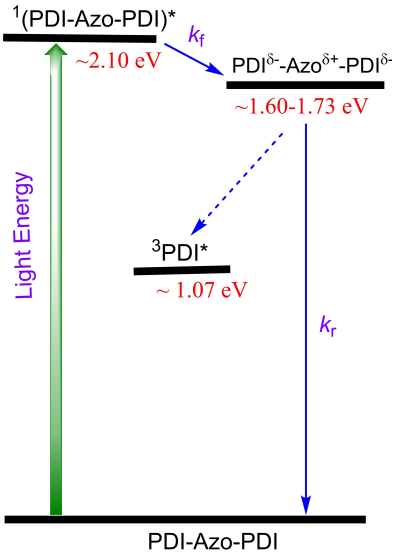

Figure 5. Energy diagram showing charge transfer processes in the triads upon photoexcitation in benzonitrile. Solid arrow – most likely process. Dashed arrow – less likely process.

from such a diagram. Importantly, a high potential charge transfer state of ~1.60–1.73 eV was possible to envision. Consequently, the charge transfer state could directly relax to the ground state or could populate the ^{3}PDI* state. It may also be mentioned here that the S_1 state of trans-isomer of azobenzene is known to be weakly fluorescent ($\Phi_f \sim 10^{-6}$) with emission in the 665 nm region.[18] Energy transfer from ^{1}PDI* to azobenzene is, therefore, a possibility. However, neither the steady-state results nor the transient data (see below) were supportive of this mechanism. Hence, contributions from such a quenching pathway are considered minimal. To unravel these mechanistic aspects, femtosecond transient absorption (fs-TA) spectral studies were performed in benzonitrile, and the findings are summarized below.

To help interpret the transient spectral data, the spectra of oxidized and reduced triads, dyads, and the control monomers were generated either by spectroelectrochemical or chemical oxidation/reduction methods. This was needed as the PDI used in the present study is different from traditionally used PDI derivatives due to strong ground state push-pull interactions. Spectral changes during the first electrochemical reduction of **Triad 2** are shown in Figure 6 while spectra for oxidized and reduced species, obtained by chemical methods for **Dyad 1**, **Dyad 2**, **Triad 1**, and **Triad 2** are shown in Figures S15 and S16. Diminished peak intensities of the neutral compound accompanied by new peaks at 502, 577, and 930 nm were witnessed for the one-electron reduced product of **Triad 2**. Isosbestic points at 387, 487, and 718 nm were also observed. The intense near-IR peak centered around 930 nm could be attributed to intervalence charge transfer (IVCT) wherein the odd electron of partially reduced triad, PDI$^{\cdot-}$-Azo-PDI, could undergo fast electron exchange between the PDI entities revealing a new optical transition.[19] However, such a near-IR peak was also present in the case of **Dyad 1** and **Dyad 2** confirming that it is due to absorption of the reduced PDI$^{\cdot-}$ moiety and not because of intervalence transition (see Figure S15). During oxidation, the diminished intensity of the initial bands accompanied by new peaks at 398, 435, 531, and 527 nm were observed, and such a trend was apparent for the other triad and dyads (See Figures S15 and S16).

Fs-TA spectra for the control **PDI 1**, lacking either the amino- or diaminoazobenzene, is shown in Figure 7. The instantaneously formed ^{1}PDI* revealed excited-state absorptions (ESA) at 502, 614, 702, 738, 835, and 941 nm. In addition, negative peaks at 487, 736, 580, and 628 nm were present. By comparison with the earlier discussed absorption and

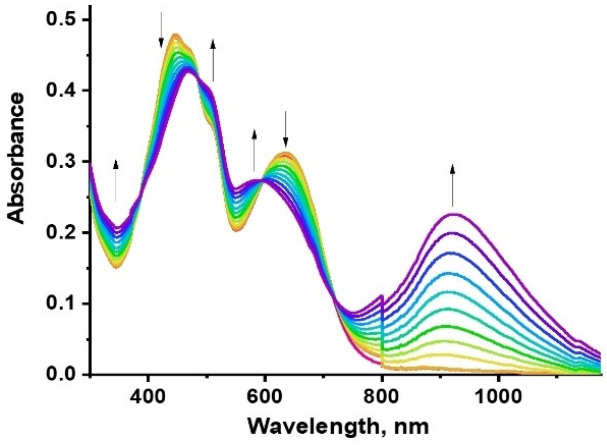

Figure 6. Spectral changes, observed during the first electro-reduction of **Triad 2** in benzonitrile containing 0.2 M (TBA)ClO_4. $E_{appl} = -0.43$ V vs. Ag/AgCl.

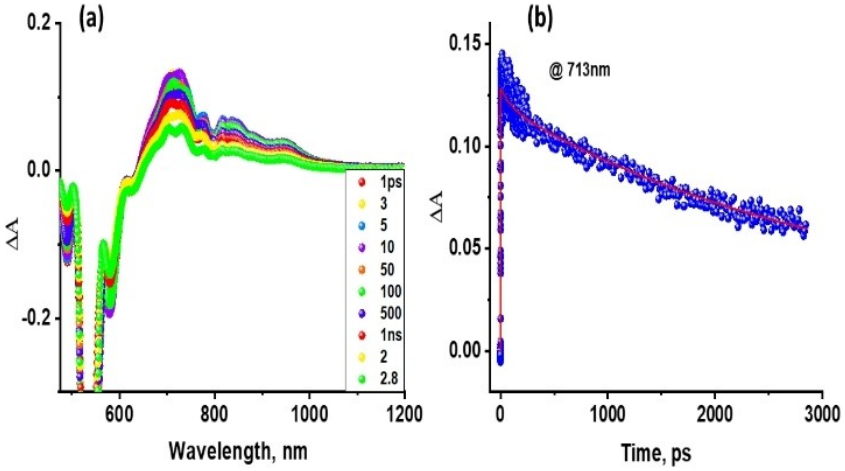

Figure 7. Fs-TA spectra at the indicated delay times of **PDI 1** in benzonitrile, excited at 535 nm. The decay profile of the 713 nm peak is shown at the right-hand panel.

fluorescence spectra, the first two peaks (487 and 736 nm) were ascribed to ground state bleach (GSB) and the last two (580 and 628 nm) to stimulated emission (SE). The central ESA peak at 738 nm had contributions from both GSB and SE. Decay of ESA peaks and the recovery of GSB and SE peaks were slow (see decay profile at the right-hand panel), consistent with its relatively long-lived singlet lifetime being 4.2 ns. Similar results were also obtained for control **PDI 2**.

Interestingly, **Dyad 1** and **Dyad 2**, having either the amino-phenyl or aminoazobenzene entities at the bay position, revealed charge transfer upon photoexcitation. For these molecules, the transient spectral features shown in Figure 8 were much different from those of monomeric **PDI 1** and **PDI 2**. In the case of **Dyad 1**, the instantaneously formed ^{1}PDI* revealed ESA peaks at 509, 550, 678, and 725 nm. In addition, a broad peak spanning the 700–900 nm region was observed (see spectrum at 1 ps). Based on the earlier discussed spectra of radical cation and radical anion species (see Figure S15), this spectrum can be attributed to the charge transfer state, $PDI^{\delta-}$-$Amino^{\delta+}$. The time profile of the near-IR peak is shown in

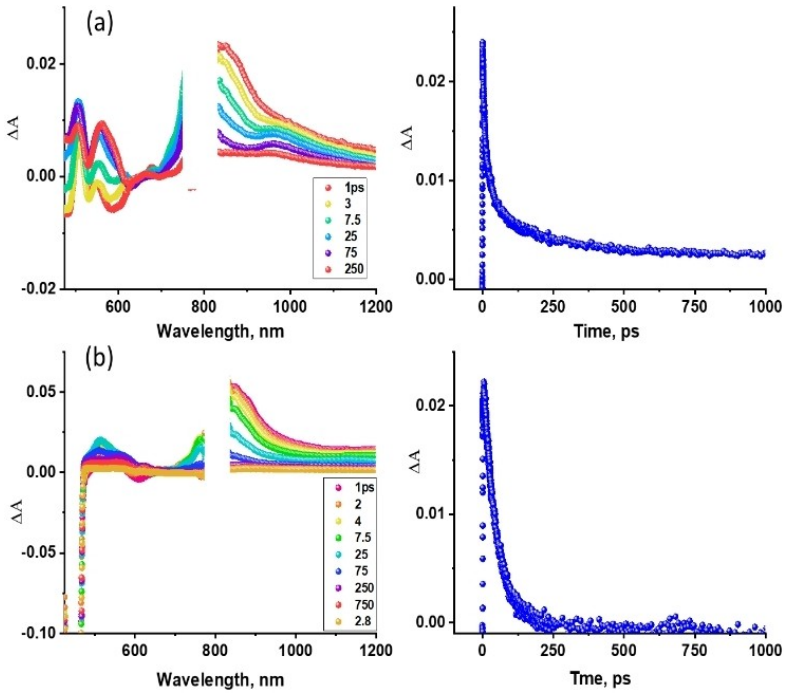

Figure 8. Fs-TA spectra at the indicated delay times for (a) **Dyad 1** (λ_{ex} = 450 nm), and (b) **Dyad 2** (λ_{ex} = 450 nm) in benzonitrile. The time profiles of the charge transfer peak monitored at 843 nm for **Dyad 1** and 840 nm for **Dyad 2** are shown at the respective right-hand panels. The break in the 800 nm range is due to visible to near-IR detector change.

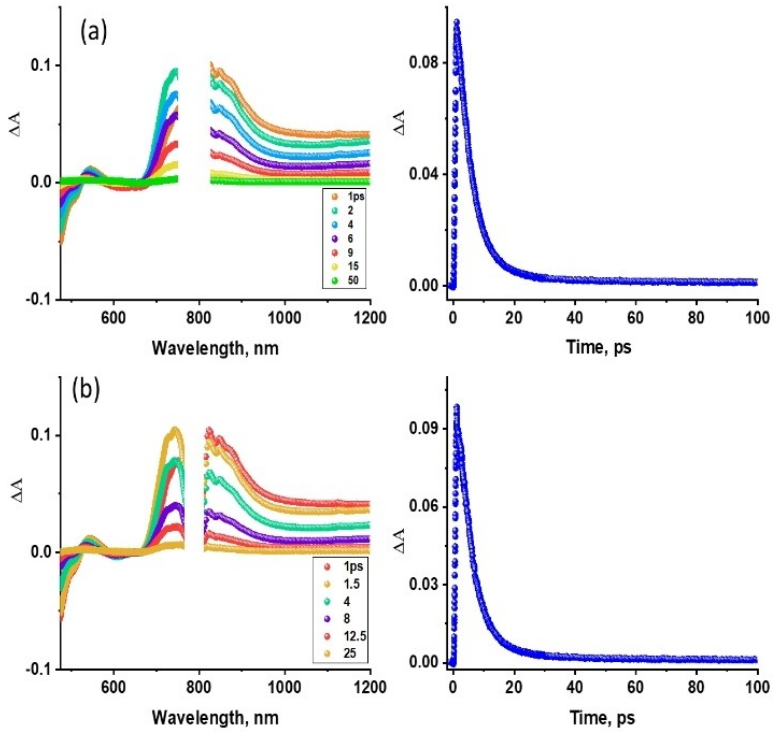

Figure 9. Fs-TA spectra at the indicated delay times of (a) **Triad 1** (λ_{ex} = 447 nm) and (b) **Triad 2** (λ_{ex} = 447 nm) in benzonitrile. The time profiles of the charge transfer peak monitored at 840 nm for **Triad 1** and 843 nm for **Triad 2** are shown in the respective right-hand panels.

Figure 8a right-hand panel. Although the majority of the decay was completed within the first 500 ps, a small long-lived component covering the entire delay time of 3 ns was observed although the origin of this spectral trend is not clear at this point.

Similar spectral features were also observed in the case of **Dyad 2** having an aminoazobenzene donor group, as shown in Figure 8b. At an early delay time of 1 ps, a well-developed broad near-IR peak at the 840–900 nm region was obvious supporting the occurrence of excited-state charge transfer. The time profile shown at the right-hand side of Figure 8b revealed the complete disappearance of the transient peaks by about 250 ps.

Finally, in the case of **Triad 1** and **Triad 2**, the transient spectral features were more or less similar to that observed for **Dyad 2**, however, with notable differences as shown in Figure 9. First, the spectral coverage of the instantaneously formed in $PDI^{\delta-}$-$Azo^{\delta+}$-$PDI^{\delta-}$ quadrupolar charge transfer state peaks was slightly blue-shifted covering the 650–1000 nm range. Second, the relaxation of the charge transfer state was much faster, that is, within about 20 ps most of the signal disappeared (see the decay profile of charge transfer peak on the right-hand panel). Additionally, the decay of the transient peaks did not produce any new signals representing ^{3}PDI* suggesting that the charge transfer state recombines directly to the ground state or signals corresponding to ^{3}PDI* are too weak to detect. Changing the excitation wavelength to the visible peak maximum also revealed such a spectral trend (see Figure S17). From the growth and decay of the near-IR charge transfer signal (for decay profiles see right-hand panels), rate constants were determined, as given in Table 2. It may be mentioned here that in the case of A–D–A triads, the transient $A^{\delta-}$-$D^{\delta+}$-$A^{\delta-}$ quadrupolar charge transfer states are known to yield A–D^+–$A^{\cdot-}$ charge-separated states, especially in charge stabilizing polar solvents[20] via the process of symmetry breaking.[21] The transient data presented here did not support such a transformation in the currently studied triads.

An examination of data given in Table 2 reveals the following: In the case of both dyads and triads, the charge transfer processes occur within the first few picoseconds and are limited by instrument response function (IRF). Under such circumstances, it is safer to conclude that the forward rate of charge transfer, k_f is closer or higher than 10^{12} s^{-1}. Charge recombination on the other hand depends on the type of donor-acceptor system. In the case of the dyads where dipolar PDI^{δ}-$Azo^{\delta+}$ charge transfer state is formed, the charge recombination was relatively slow with k_r values in the order of 10^{10} s^{-1}.

Table 2. Forward (k_f) and reverse (k_r) charge transfer rate constants for the investigated compounds in benzonitrile.

Compound	λ_{ex}, nm	k_f, s^{-1}	k_r, s^{-1}
Dyad 1	450	$\sim 10^{12}$	1.11×10^{10}
	600	$\sim 10^{12}$	1.33×10^{10}
Dyad 2	450	$\sim 10^{12}$	1.98×10^{10}
Triad 1	450	$\sim 10^{12}$	1.53×10^{11}
	639	$\sim 10^{12}$	1.66×10^{11}
Triad 2	450	$\sim 10^{12}$	1.56×10^{11}
	639	$\sim 10^{12}$	1.66×10^{11}

Interestingly, in the case of triads, where $PDI^{\delta-}$-$Azo^{\delta+}$-$PDI^{\delta-}$ quadrupolar charge transfer states are formed, the k_r values were an order of magnitude higher meaning a faster charge recombination process. That is, compounds with the ability to form quadrupolar charge transfer states revealed accelerated charge recombination compared to those compounds forming dipolar charge transfer states This could be attributed to statistical factors. Changing the excitation wavelength did not drastically alter both k_f and k_r values retaining similar trends between the dyads and triads.

Conclusions

In summary, the covalent attachment of aminoazobenzene or aminophenyl groups at the bay positions of PDI resulted in new types of dyads and triads. Due to the presence of strong push-pull effects, modulation of absorption spectral features extending the optical coverage into the entire visible region and charge transfer emission in the near-IR region was witnessed. Using fluorescence-spectroelectrochemistry, charge transfer reversal was possible wherein the PDI fluorescence recovery upon one-electron oxidation of the triad was possible. The formation of dipolar $PDI^{\delta-}$-$Azo^{\delta+}$ in the dyads and quadrupolar $PDI^{\delta-}$-$Azo^{\delta+}$-$PDI^{\delta-}$ in the triads was possible to demonstrate by constructing charge transfer state density difference, and the frontier orbitals on DFT optimized structures. The established energy diagrams revealed the thermodynamic feasibility of charge transfer. Femtosecond transient absorption spectral studies, excited at both absorption peak maxima revealed ultrafast events wherein the forward charge transfer events occurred within a few ps due to the proximity of the donor and acceptor entities. Interestingly, the charge recombination rate constants were structure dependent. That is, faster k_r in the case of triads compared to dyads was witnessed. Additionally, the charge transfer states relaxed directly to the ground state without populating the ^{3}PDI* in both dyads and triads or formation of dipolar PDI-Azo^+-PDI^- charge-separated state in the case of triads. The significance of diaminoazobenzene in promoting wide-band capture and ultrafast charge transfer in PDI-azobenzene-derived dyads and triads are the outcomes of this study.

Experimental Section

General methods: Solvents and reagents were obtained from commercial sources and used as received. Column chromatography: SiO_2 (40–63 μm). TLC plates coated with SiO_2 60F254 were visualized by UV light. NMR spectra were recorded using a Bruker AC300 spectrometer. The solvents for spectroscopic studies were of spectroscopic grade and used as received. UV-vis spectra were measured with a Helios Gamma spectrophotometer. IR spectra were recorded with a Nicolet Impact 400D spectrophotometer. High-resolution mass spectra were obtained from a Bruker Reflex II matrix-assisted laser desorption/ionization-time of flight (MALDI-TOF) using dithranol as the matrix.

At UNT, the UV-visible spectral measurements were carried out with a Jasco V670 UV-visible-near IR spectrophotometer. The fluorescence emission was monitored by using a Horiba Yvon Nanolog coupled with time-correlated single-photon counting with nanoLED excitation sources. A right-angle detection method was used. Differential pulse and cyclic voltammograms were recorded on an EG&G 263A electrochemical analyzer using a three-electrode system. A platinum button electrode was used as the working electrode. A platinum wire served as the counter electrode and an Ag/AgCl electrode was used as the reference electrode. Ferrocene/ferrocenium redox couple was used as an internal standard. All the solutions were purged before electrochemical and spectral measurements using argon gas.

The spectroelectrochemical study was performed by using a cell assembly (SEC-C) supplied by ALS Co., Ltd. (Tokyo, Japan). This assembly comprised of a Pt counter electrode, a 6 mm Pt Gauze working electrode, and an Ag/AgCl reference electrode in a 1.0 mm path length quartz cell. The optical transmission was limited to 6 mm covering the Pt Gauze working electrode. Spectra were recorded by applying a potential 80 mV past the potential of a given oxidation or reduction process and continued until no additional changes were observed. The final spectrum of the radical anion and radical cation of a given compound was averaged and subtracted from the neutral compound to resemble the differential absorption spectrum of charge separation product from transient absorption studies.

Femtosecond transient absorption spectroscopy: Experiments were performed using an ultrafast femtosecond laser source (Libra) by Coherent incorporating a diode-pumped, mode-locked Ti: sapphire laser (Vitesse), and a diode-pumped intracavity doubled Nd:YLF laser (Evolution) to generate a compressed laser output of 1.45 W. For optical detection, a Helios transient absorption spectrometer coupled with a femtosecond harmonics generator, both provided by Ultrafast Systems LLC, was used. The sources for the pump and probe pulses were derived from the fundamental output of Libra (Compressed output 1.45 W, pulse width 100 fs) at a repetition rate of 1 kHz; 95% of the fundamental output of the laser was introduced into a TOPAS-Prime-OPA system with a 290–2600 nm tuning range from Altos Photonics Inc., (Bozeman, MT), while the rest of the output was used for generation of a white light continuum. Kinetic traces at appropriate wavelengths were assembled from the time-resolved spectral data. Data analysis was performed using Surface Xplorer software supplied by Ultrafast Systems. All measurements were conducted in degassed solutions at 298 K. The estimated error in the reported rate constants is ±10%.

Synthesis

4,4′-Bis[N,N′-di(hexylheptyl)perylene-3′′,4′′:9′′,10′′-tetracarboxidiimide-1′′-ylamino]azobenzene (Triad 1)

4,4′-Diaminoazobenzene (21 mg, 0.1 mmol) and TBAF (1 M in THF, 1.5 mL, 1.5 mmol) were added to a solution of *N*,*N*′-di(hexylheptyl)-3,4:9,10-perylenetetracarboxydiimide, **PDI 1**, (189 mg, 0.25 mmol) in dry THF (0.2 mL). The reaction was refluxed 24 h under argon atmosphere and, after cooling, it was extracted with dichloromethane and washed with water. The organic layer was dried over anhydrous sodium sulfate, filtered and evaporated. Purification was carried out by silica gel column chromatography using dichloromethane:acetone 150:1 as eluent to give compound **Triad 1** as a green powder (90 mg, 56%).

^{1}H NMR (300 MHz, $C_2D_2Cl_4$, 70 °C): δ 9.21 (d, J = 8.29 Hz, 2H), 8.75 (m, 4H), 8.63 (m, 8H), 8.02 (d, J = 8.67 Hz, 4H), 7.28 (d, J = 8.73 Hz, 4H),

6.83 (s, 2H), 5.18 (m, 4H), 2.24 (m, 8H), 1.93 (m, 8H), 1.29 (m, 64H), 0.89 ppm (br, 24H). ^{13}C NMR (75 MHz, $C_2D_2Cl_4$, 70 °C): δ 148.72, 142.91, 140.65, 134.60, 133.71, 129.47, 128.64, 127.28, 125.96, 124.88, 123.80, 122.88, 121.92, 118.06, 54.83, 54.60, 32.30, 31.53, 29.47, 28.97, 26.79, 22.36, 13.81 ppm. MS MALDI-TOF: *m/z* calcd for $C_{112}H_{132}N_8O_8$ $[M]^-$ 1717.0162; found: 1717.0180. IR (KBr): ν 3318, 2924, 2854, 1697, 1656, 1591, 1503, 1457, 1411, 1331, 1267, 1249, 1176, 1151, 844, 810 cm^{-1}; UV-vis (CH_2Cl_2): λ_{max} [nm (log ε)]: 435 (4.7), 625 (4.6).

4,4′-Bis[N,N′-di(ethylpropyl)perylene-3′′,4′′:9′′,10′′-tetracarboxidiimide −1′′-ylamino]azobenzene (Triad 2)

4,4′-Diaminoazobenzene (42 mg, 0.2 mmol) and TBAF (1 M in THF, 3 mL, 3 mmol) were added to a solution of *N,N′*-di(ethyl propyl)-3,4:9,10-perylenetetracarboxydiimide, **PDI 2**, (266 mg, 0.5 mmol) in dry toluene (0.4 mL). The reaction was refluxed 24 h under argon atmosphere and, after cooling, it was extracted with dichloromethane and washed with water. The organic layer was dried over anhydrous sodium sulfate, filtered, and evaporated. Purification was carried out by silica gel column chromatography using dichloromethane:acetone 100:5 as eluent to give compound **Triad 2** as a green powder (121 mg, 48%).

^{1}H NMR (300 MHz, $C_2D_2Cl_4$, 70 °C): δ 9.19 (d, J = 8.29 Hz, 2H), 8.74 (m, 4H), 8.63 (m, 6H), 8.56 (d, J = 8.27, 2H), 8.02 (d, J = 8.75 Hz, 4H), 7.27 (d, J = 8.82 Hz, 4H), 6.82 (s, 2H), 5.06 (m, 4H), 2.25 (m, 8H), 2.00 (m, 8H), 0.99 (t, J = 7.4 Hz, 12H), 0.97 ppm (t, J = 7.4 Hz, 12H); ^{13}C NMR (75 MHz, $C_2D_2Cl_4$, 70 °C): δ 164.31, 163.68, 143.18, 140.95, 134.82, 131.64, 131.32, 129.29, 127.90, 125.07, 124.60, 124.24, 123.99, 123.53, 123.13, 122.28, 122.07, 118.23, 58.06, 57.83, 25.19, 11.45 ppm; MS MALDI-TOF: *m/z* calcd for $C_{80}H_{68}N_8O_8$ $[M]^-$ 1269.5232; found: 1269.5499. IR (KBr): ν 3214, 2932, 2851, 1689, 1643, 1590, 1491, 1409, 1334, 1264, 1088, 803 cm^{-1}. UV-vis (CH_2Cl_2): λmax/nm (log ε): 435 (4.5), 608 (4.3).

N,N′-Di(hexylheptyl)-1-(4′-phenylazophenylamino)-3,4:9,10-perylenetetracarboxydiimide (Dyad 2)

4-Aminoazobenzene (190 mg, 0.96 mmol) and TBAF (1 M in THF, 1.5 mL, 1.5 mmol) were added to a solution of *N,N′*-di(hexylheptyl)-3,4:9,10-perylenetetracarboxydiimide, **PDI 1**, (180 mg, 0.25 mmol) in dry THF (0.2 mL). The reaction was refluxed 24 h under argon atmosphere and, after cooling, it was extracted with dichloromethane and washed with water. The organic layer was dried over anhydrous sodium sulfate, filtered, and evaporated. Purification was carried out by silica gel column chromatography using dichloromethane as an eluent to give compound **Dyad 2** as a green powder (87 mg, 38%).

^{1}H NMR (300 MHz, $C_2D_2Cl_4$, 70 °C): δ 9.15 (d, J = 8.25 Hz, 1H), 8.58 (m, 6H), 7.98 (d, J = 8.55 Hz, 2H), 7.88 (d, J = 7.05 Hz, 2H), 7.50 (m, 3H), 7.25 (d, J = 8.65 Hz, 2H), 6.86 (s, 1H), 5.11 (br, 2H), 2.15 (br, 4H), 1.76 (br, 4H), 1.22 (br, 32H), 0.82 ppm (br, 12H); ^{13}C NMR (75 MHz, $C_2D_2Cl_4$, 70 °C): δ 164.29, 163.86, 152.75, 148.28, 143.65, 140.71, 134.84, 133.86, 130.71, 129.49, 129.20, 128.75, 127.26, 126.11, 125.34, 124.16, 123.10, 122.76, 122.24, 122.14, 117.95, 117.54, 117.17, 54.74, 32.39, 31.85, 31.83, 29.31, 27.06, 22.73, 22.72, 14.26 ppm; MS MALDI-TOF: *m/z* calcd for $C_{62}H_{171}N_5O_4$ $[M]^-$ 949.5506; found: 949.5446; IR (KBr): ν 3420, 2950, 2917, 2852, 1691, 1654, 1581, 1507, 1413, 1332, 1148, 813, 743 cm^{-1}; UV-vis (CH_2Cl_2): λmax/nm (log ε): 392 (4.4), 457 (4.3), 484 (4.2), 593 (4.2).

Supporting Information

Contains article, experimental and synthetic details ^{1}H and ^{13}C NMR and HRMS spectra of all the new compounds, differential pulse voltammograms, computational results and additional transient spectral data.

Acknowledgements

This research was supported by the US-National Science Foundation (2000988 to FD) and by the European Regional Development Fund "A way to make Europe" and the Spanish Ministerio de Ciencia e Innovación/Agencia Estatal de Investigación (PID2019-109200GB-I00 to FF-L). The computational work was completed at the Holland Computing Center of the University of Nebraska, which receives support from the Nebraska Research Initiative.

Conflict of Interest

The authors declare no conflict of interest.

Data Availability Statement

The data that support the findings of this study are available from the corresponding author upon reasonable request.

Keywords: diaminoazobenzene · fluorescence spectroelectrochemistry · perylenediimide-azobenzene triad · quadrupolar charge transfer · ultrafast spectroscopy

[1] a) M. R. Wasielewski, *Acc. Chem. Res.* **2009**, *42*, 1910; b) D. Gust, T. A. Moore, A. L. Moore, *Acc. Chem. Res.* **2009**, *42*, 1890; c) N. Armaroli, V. Balzani, *Angew. Chem. Int. Ed.* **2007**, *46*, 52; *Angew. Chem.* **2007**, *119*, 52; d) V. Sgobba, D. M. Guldi, *Chem. Soc. Rev.* **2009**, *38*, 165; e) H. Imahori, S. Fukuzumi, *Adv. Funct. Mater.* **2004**, *14*, 525; f) S. Fukuzumi, *Phys. Chem. Chem. Phys.* **2008**, *10*, 2283; g) G. Bottari, G. de la Torre, D. M. Guldi, T. Torres, *Chem. Rev.* **2010**, *110*, 6768; h) F. D'Souza, O. Ito, *Chem. Soc. Rev.* **2012**, *41*, 86.

[2] S. A. Wolf, D. D. Awschalom, R. A. Buhrman, J. M. Daughton, S. von Molnar, M. L. Roukes, A. Y. Chtchelkanova, D. M. Treger, *Science* **2001**, *295*, 1488.

[3] B. K. Rugg, M. D. Krzyaniak, B. T. Phelan, M. A. Ratner, R. M. Young, M. R. Wasielewski, *Nat. Chem.* **2019**, *11*, 981.

[4] a) *Intramolecular Charge Transfer: Theory and Applications*, R. Misra, S. P. Bhattachaaryya, Wiley-VCH Verlag, **2018**; b) *Charge and Energy Transfer Dynamics in Molecular Systems*, 3rd ed. V. May, O. Kuhn, Wiley-VCH, **2011**.

[5] W. Herbst, K. Hunger, *Industrial Organic Pigments: Production, Properties*, Applications, 2nd ed., Wiley-VCH, Weinheim, **1997**.

[6] a) F. Würthner, M. Stolte, *Chem. Commun.* **2011**, *47*, 5109; b) Z. Liu, G. Zhang, Z. Cai, X. Chen, H. Luo, Y. Li, J. Wang, D. Zhang, *Adv. Mater.* **2014**, 26, 6965; c) F. Würthner, C. R. Saha-Möller, B. Fimmel, S. Ogi, P. Leowanawat, D. Schmidt, *Chem. Rev.* **2016**, *116*, 962; d) I. K. Sideri, Y. Jang, J. Garces-Garces, A. Sastre-Santos, R. Canton-Vitoria, R. Kitaura, F. Fernandez-Lazaro, F. D'Souza, N. Tagmatarchis, *Angew. Chem. Int. Ed.* **2021**, *60*, 9120.

[7] a) Y. Liu, S. Gao, L. Yang, Y.-L. Liu, X.-M. Liang, F. Ye, Y. Fu, *Front. Chem.* **2020**, *8*, 702; b) S. Chen, Z. Xue, N. Gao, X. Yang, L. Zang, *Sensors* **2020**, *20*, 917; c) P. Calvo-Gredilla, J. García-Calvo, J. V. Cuevas, T. Torroba, J.-L.

Pablos, F. C. García, J.-M. García, N. Zink-Lorre, E. Font-Sanchis, Á. Sastre-Santos, F. Fernández-Lázaro, *Chem. Eur. J.* **2017**, *23*, 13973.
[8] a) N. Zink-Lorre, E. Font-Sanchis, Á. Sastre-Santos, F. Fernández-Lázaro, *Chem. Commun.* **2020**, *56*, 3824; b) F. Fernández-Lázaro, N. Zink-Lorre, Á. Sastre-Santos, *J. Mater. Chem. A* **2016**, *4*, 9336; c) E. Kozma, M. Catellani, *Dyes Pigm.* **2013**, *98*, 160; d) G. Zhang, J. Feng, X. Xu, W. Ma, Y. Li, Q. Peng, *Adv. Funct. Mater.* **2019**, *29*, 1906587.
[9] a) A. Nowak-Krol, F. Würthner, *Org. Chem. Front.* **2019**, *6*, 1272; b) F. Zhang, Y. Ma, Y. Chi, H. Yu, Y. Li, T. Jiang, X. Wei, J. Shi, *Science Reports* **2018**, *8*, 8208.
[10] a) G. S. Hartley, *Nature* **1937**, *140*, 281; b) T. Schultz, J. Quenneville, B. Levine, A. Toniolo, T. J. Martínez, S. Lochbrunner, M. Schmitt, J. P. Shaffer, M. Z. Zgierski, A. Stolow, *J. Am. Chem. Soc.* **2003**, *125*, 8098; c) H. D. Bandara, S. C. Burdette, *Chem. Soc. Rev.* **2012**, *41*, 1809; d) A. A. Beharry, G. A. Woolley, *Chem. Soc. Rev.* **2011**, *40*, 4422; e) J. Garcia-Amoros, D. Velasco, *Beilstein J. Org. Chem.* **2012**, *8*, 1003; f) Y. Kim, A. Garcia-Lekue, D. Sysoiev, T. Frederiksen, U. Groth, E. Scheer, *Phys. Rev. Lett.* **2012**, *109*, 226801.
[11] For imide-linked azobenzene see: W. Ling, X. Cheng, T. Miao, S. Zhang, W. Zhang, X. Zhu, *Polymer* **2019**, *11*, 1143.
[12] N. Zink-Lorre, S. Seetharaman, D. Gutiérrez-Moreno, F. Fernández-Lázaro, P. A. Karr, F. D'Souza, *Chem. Eur. J.* **2021**, *27*, 14996–15005.
[13] a) D. Pinjari, A. Z. Alsaleh, Y. Patil, R. Misra, F. D'Souza, *Angew. Chem. Int. Ed.* **2020**, 132, 23905; b) I. S. Yadav, A. Z. Alsaleh, R. Misra, F. D'Souza, *Chem. Sci.* **2021**, 12, 1109; c) F. Khan, Y. Jang, Y. Patil, R. Misra, F. D'Souza, *Angew. Chem. Int. Ed.* **2021**, *60*, 20518–20527; d) M. K. Chahal, A. Liyanage, A. Z. Alsaleh, P. A. Karr, J. P. Hill, F. D'Souza, *Chem. Sci.* **2021**, *12*, 4925.
[14] a) S. Demmig, H. Langhals, *Chem. Ber.* **1988**, *121*, 225–230; b) D. Gutiérrez-Moreno, Á. Sastre-Santos, F. Fernández-Lázaro, *Org. Chem. Front.* **2019**,*6*, 2488.
[15] L. Martín Gomis, R. Díaz-Puertas, S. Seetharaman, P. A. Karr, F. Fernández-Lázaro, F. D'Souza, Á. Sastre-Santos, *Chem. Eur. J.* **2020**, *26*, 4822.
[16] R. Canton-Vitoria, H. B. Gobeze, V. M. Blas-Ferrando, J. Ortiz, Y. Jang, F. Fernandez-Lazaro, A. Sastre-Santos, Y. Nakanishi, H. Shinohara, F. D'Souza, N. Tagmatarchis, *Angew. Chem. Int. Ed.* **2019**, *58*, 5712.
[17] *Gaussian 16*, M. J. Frisch, G. W. Trucks, H. B. Schlegel, G. E. Scuseria, M. A. Robb, J. R. Cheeseman, G. Scalmani, V. Barone, B. Mennucci, G. A. Petersson, H. Nakatsuji, M. Caricato, X. Li, H. P. Hratchian, A. F. Izmaylov, J. Bloino, G. Zheng, J. L. Sonnenberg, M. Hada, M. Ehara, K. Toyota, R. Fukuda, J. Hasegawa, M. Ishida, T. Nakajima, Y. Honda, O. Kitao, H. Nakai, T. Vreven, J. A. Montgomery Jr., J. E. Peralta, F. Ogliaro, M. Bearpark, J. J. Heyd, E. Brothers, K. N. Kudin, V. N. Staroverov, R. Kobayashi, J. Normand, K. Raghavachari, A. Rendell, J. C. Burant, S. S. Iyengar, J. Tomasi, M. Cossi, N. Rega, J. M. Millam, M. Klene, J. E. Knox, J. B. Cross, V. Bakken, C. Adamo, J. Jaramillo, R. Gomperts, R. E. Stratmann, O. Yazyev, A. J. Austin, R. Cammi, C. Pomelli, J. W. Ochterski, R. L. Martin, K. Morokuma, V. G. Zakrzewski, G. A. Voth, P. Salvador, J. J. Dannenberg, S. Dapprich, A. D. Daniels, Ö. Farkas, J. B. Foresman, J. V. Ortiz, J. Cioslowski, D. J. Fox, *Gaussian, Inc.*, Wallingford, CT, USA, Willingford, CT, USA.
[18] H. Satzger, S. Sporlein, C. Root, J. Wachtveitl, W. Zinth, P. Gilch, *Chem. Phys. Lett.* **2003**, *372*, 216–223.
[19] a) J. Hankache, O. S. Wenger, *Chem. Rev.* **2011**, *111*, 5138; b) A. Heckmann, C. Lambert, *Angew. Chem. Int. Ed.* **2012**, *51*, 326.
[20] a) B. Dereka, A. Rosspeintner, M. Krzeszewski, D. T. Gryko, E. Vauthey, *Angew. Chem. Int. Ed.* **2016**, *55*, 15624–15628; *Angew. Chem.* **2016**, *128*, 15853–15857; b) B. Dereka, A. Rosspeintner, R. Stezycki, C. Ruckebusch, D. T. Gryko, E. Vauthey, *J. Phys. Chem. Lett.* **2017**, *8*, 6029–6034.
[21] a) V. Markovic, D. Villamaina, I. Barabanov, L. M. Lawson Daku, E. Vauthey, *Angew. Chem. Int. Ed.* **2011**, *123*, 7738–7740; b) A. Aster, G. Licari, F. Zinna, E. Brun, T. Kumpulainen, E. Tajkhorshid, J. Lacour, E. Vauthey, *Chem. Sci.* **2019**, *10*, 10629–10639; c) E. Vauthey, *ChemPhysChem* **2012**, *13*, 2001–2011; d) J. M. Giaimo, A. V. Gusev, M. R. Wasielewski, *J. Am. Chem. Soc.* **2002**, *124*, 8530–8531; e) R. M. Young, M. R. Wasielewski, *Acc. Chem. Res.* **2020**, *53*, 1957–1968; f) C. E. Ramirez, S. Chen, N. E. Powers-Riggs, I. Schlesinger, R. M. Young, M. R. Wasielewski, *J. Am. Chem. Soc.* **2020**, *142*, 18243–18250; g) K. Miyata, Y. Kurashige, K. Watanabe, T. Sugimoto, S. Takahashi, S. Tanaka, J. Takeya, T. Yanai, Y. Matsumoto, *Nat. Chem.* **2017**, *9*, 983; h) T. Kim, J. Kim, H. Mori, S. Park, M. Lim, A. Osuka, D. Kim, *Phys. Chem. Chem. Phys.* **2017**, *19*, 13970–13977; i) B. Carlotti, E. Benassi, A. Spalletti, C. G. Fortuna, F. Elisei, V. Barone, *Phys. Chem. Chem. Phys.* **2014**, *16*, 13984–13994; j) . Kong, W. Zhang, G. Li, D. Huo, Y. Guo, X. Niu, Y. Wan, B. Tang, A. Xia, *J. Phys. Chem. Lett.* **2020**, *11*, 10329–10339; k) M. T. Whited, N. M. Patel, S. T. Roberts, K. Allen, P. I. Djurovich, S. E. Bradforth, M. E. Thompson, *Chem. Commun.* **2012**, *48*, 284–286; l) J. H. Golden, L. Estergreen, T. Porter, A. C. Tadle, D. Sylvinson M. R, J. W. Facendola, C. P. Kubiak, S. E. Bradforth, M. E. Thompson, *ACS Appl. Energ. Mater.* **2018**, *1*, 1083–1095; m) M. Kellogg, A. Akil, D. S. M. Ravinson, L. Estergreen, S. E. Bradforth, M. E. Thompson, *Faraday Discuss.* **2019**, *216*, 379–394.

Manuscript received: December 23, 2021
Accepted manuscript online: January 21, 2022
Version of record online: ■■, ■■■

RESEARCH ARTICLE

Efficient quadrupolar charge transfer in diaminoazobenzene-bridged perylenediimide triads resulted in wide-band light capture. Charge-transfer emission was also possible to observe, and by fluorescence-spectroelectrochemistry it was possible to revert this phenomenon. Ultrafast quadrupolar charge transfer was confirmed by computational and femtosecond pump-probe spectroscopy in these triads.

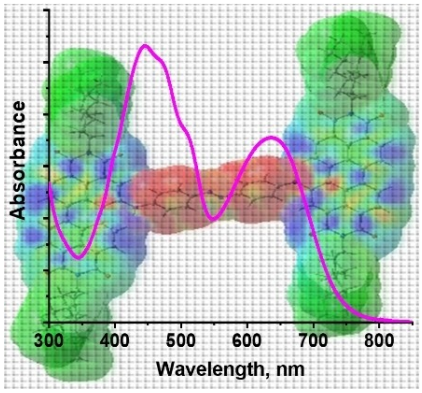

Dr. S. Seetharaman, Dr. N. Zink-Lorre, Dr. D. Gutiérrez-Moreno, Prof. Dr. P. A. Karr, Prof. Dr. F. Fernández-Lázaro, Prof. Dr. F. D'Souza**